Comets in the Near-Earth Object Population

by

Francesca E. DeMeo

Submitted to the Department of Earth, Atmospheric and Planetary Sciences

in Partial Fulfillment of the Requirements for the Degree of

Bachelor of Science in Earth, Atmospheric, and Planetary Sciences

at the Massachusetts Institute of Technology

May 12, 2006 [June 2006]

Author _____ Signature redacted _____

Department of Earth, Atmospheric and Planetary Sciences
May 1, 2006

Certified by _____ Signature redacted _____

Professor Richard P. Binzel
Thesis Supervisor

Accepted by _____ Signature redacted _____

Professor Samuel Bowring
Chair, Committee on Undergraduate Program

Table of Contents

Comets in the Near-Earth Object Population
By
Francesca E. DeMeo

Submitted to the
Department of Earth, Atmospheric and Planetary Sciences

May 1, 2006

In Partial Fulfillment of the Requirements for the Degree of
Bachelor of Science in Earth, Atmospheric, and Planetary Sciences

ABSTRACT

Because the lifespan of near-Earth objects (NEOs) is shorter than the age of the solar system, these objects originated elsewhere and they must have a source of re-supply. We seek to determine what fraction of the NEO population consists of dormant or extinct comets. We identify comet candidates among NEOs using three criteria: the Jovian Tisserand parameter $Tj < 3$, comet nucleus-like spectral parameters (generally linear spectra which correspond to C, D, or P taxonomic types), and low (<0.075) albedos. Out of 31 objects we sample having $Tj < 3$, we find 17 objects or approximately 55% also satisfy these comet candidate criteria. Bias corrected discovery statistics (Stuart 2003, Ph.D. thesis; Stuart & Binzel 2004, Icarus 170, 295) estimate 30% of the entire NEO population resides in orbits having a value of $Tj < 3$. Combining these two factors suggests that approximately 16% of the total NEO population has both dynamical and physical properties consistent with a cometary origin.

Thesis Supervisor: Richard P. Binzel
Title: Professor of Planetary Science

Acknowledgements

I would like to thank my advisor, Rick Binzel, for everything he has taught me and helped me with as an undergraduate and for all the opportunities he provided. I also owe a huge thanks to Andy Rivkin and Cristina Thomas, who both have always been very patient with me especially in the beginning when I had a million questions. They all were willing to take the time to help me.

Introduction

Asteroids are protoplanetary rocky bodies ranging from meters to hundreds of kilometers in diameter. These objects reside in the solar system, many in the main asteroid belt, located between Mars and Jupiter at 2 to 5 astronomical units (AU). Some asteroids called near-Earth asteroids cross or come close to Earth's orbit. These objects are interesting because of their proximity to Earth and their wide range of spectral properties. The lifespan of these near-Earth asteroids is shorter than the age of the solar system necessitating resupply from other locations in the solar system. Many of these objects are believed to originate in the main belt escaping through instabilities at the 3:1 resonance and nu6 resonances. (Wisdom, 1985) Some objects in this near-Earth population, however, have characteristics not shared by asteroids, but instead by comets. We seek to determine the fraction of comets and comet-like objects that reside in the near-Earth population.

It is important to understand the distinctions between different types of objects. We define a comet as an ice-dominated body that displays a coma or a tail when resolved through a telescope. A comet-like object (which is either a dormant or extinct comet and is referred to as a comet candidate) has the same physical and dynamical characteristics as a comet, but does not exhibit a visible coma or tail. An asteroid is an inner solar system rocky body too small to be a planet. Mars Crossers are objects with a perihelion distance between 1.3 and 1.67 AU. These objects are not considered near-Earth objects; near-Earth objects or NEOs are bodies whose orbit has a perihelion value less than 1.3 AU. These are separated further into three subcategories. Amors have perihelion distances between 1.017 and 1.3, Apollos have perihelions less than 1.017 and semi-

major axes greater than 1.017, and Atens have both a perihelion and semi-major axis less than 0.983. 1.017AU is the aphelion of Earth's orbit and 0.983 is the perihelion, which explains the boundary conditions for near-Earth object classification.

When examining these near-Earth objects, both dynamical and physical properties are significant in identifying comet-like bodies. We use three criteria: Jovian Tisserand parameter less than 3, low albedo, and linear, comet-like spectra.

Significance

Asteroids and comets are relics of the inner and outer solar system; they comprise the most pristine objects in the solar system because they have not undergone significant differentiation. Studying the composition of these objects reveals information about the earliest stages of solar system formation; studying the current locations of these objects in comparison to the formation region unveils possible evolutions of the solar system and migration paths of objects. Many NEOs are objects thrown from the main asteroid belt, but new studies suggest dormant or extinct comets may comprise a significant portion of the NEO population. It is believed that transportation of objects beyond the main belt in the outer solar system to near-Earth space is possible by perturbation. (Holman et al. 1993)

By finding the observed relative abundances of comets in the NEO population we strive to connect dynamical models of evolution to the actual solar system itself. One of the most important questions regarding the NEO population is "How did near-Earth objects arrive at their current location?" We know that there is a large variety of objects

suggesting both asteroidal and cometary source regions, and by determining the percentage of each type present in the population we can confirm the existence of migration and work toward finding the frequency of migration of objects from their initial source regions, refining our models of how these objects arrived in near-Earth space.

Method

To identify potential dormant or extinct comets we characterize our objects using both dynamical and physical properties, focusing on three criteria: the Jovian Tisserand Parameter Tj, spectral parameters, and albedo when available.

The Jovian Tisserand parameter shown in equation 1 is a conserved quantity that characterizes the strength of the gravitational interaction between Jupiter and a second body:

$$Tj = (aj/a) + 2[(1-e^2)a/aj]^{1/2}\cos(i) \qquad (1)$$

Jupiter itself has Tj = 3. Main-belt asteroids typically have Tj>3 and are unaffected by Jupiter. Objects with Tj<3 are strongly tied to Jupiter. Jupiter Family comets generally have Tisserand parameter values between 2 and 3. Halley Family comets have Tj<2. This distinction between two types of short period (T< 200 years) comets was proposed by Carusi and Valsecchi (1987). Jupiter Family comets, all with Tisserand parameters near 3, have low velocities when passing by Jupiter and therefore are strongly affected by its gravity. (Weissman et al. 2002) Near-Earth objects with Tj<3, therefore, are likely to

have cometary origins. As can be seen in Figure 1 the Tisserand values nicely differentiate objects in different locations in the solar system. The Tj=3 boundary, however, is not definite. Asteroid orbits can be altered by other bodies and become more strongly tied with Jupiter resulting in a Tj value less than three. Jupiter Family Comets, many in highly irregular orbits and with Tj values near the 3 boundary, can pass near large bodies affecting their orbits and pushing their Tj value above 3. While we recognize the limits of this barrier, for the statistical purposes of this paper we treat Tj =3 as a definitive boundary and consider only objects with values less than 3. Refer to Appendix A to see the 31 NEOs in the sample and their Tisserand values.

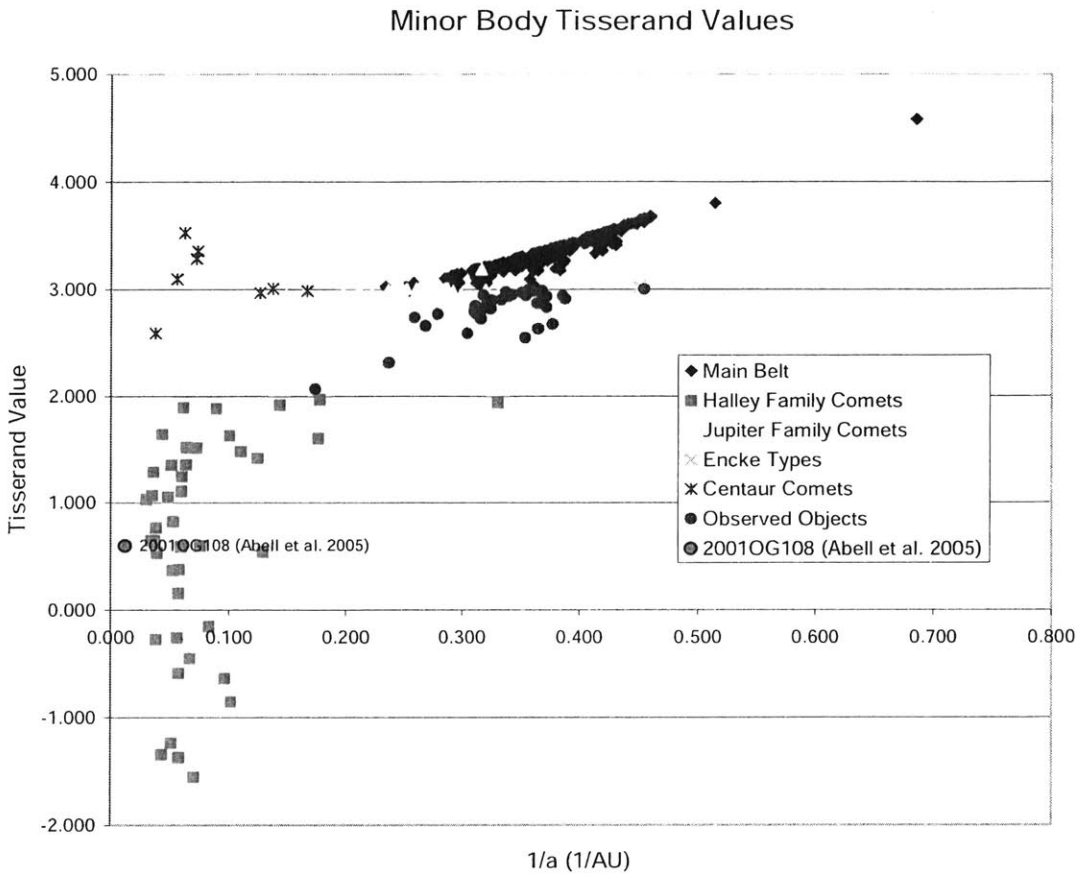

Figure 1: Plot of the inverse of the semi-major axis versus Tisserand parameter. This demonstrates the usefulness of the Tisserand parameter to distinguish between object types.

Low albedos usually determined through flux measurements at thermal infrared (5-20 microns) wavelengths, also produce measurable flux less than 2.5 microns for dark NEOs in the vicinity of 1 AU (as recognized by Lebofsky & Spencer [1989], and first reported for SpeX measurements by Abell et al. [2002; 2003]). Dark objects absorb more

light than lighter objects and heat up. If they are close enough to the sun, they will heat enough to display thermal emission at low wavelengths.

Typical comet albedos are very low, ranging from 0.02 to 0.06 as stated in Lamy et al. (2004). Typical near-Earth and main-belt asteroid albedos are above 0.1 (Delbo et al. 2003; Tedesco et al. 1989). Asteroids with thermal emission present at 2.5 microns therefore give a clear indication of a comet-like low albedo, suggesting a comet connection. For the purposes of this paper we use an albedo of 0.075 as the cutoff for "low albedo" objects.

Albedo measurements are most important for the degenerate X-type objects. The X class represents three distinct taxonomies: E, M, and P. While they all show the same featureless spectral characteristics, E-type objects have very high albedos with values greater than 0.3, M-types exhibit medium albedos usually ranging between 0.075 and 0.3, and P-type objects have extremely low albedos less than 0.075. By using albedo values we further classify as many X-types as possible. The low albedo P-types are the only objects of these three types that are considered comet candidates.

For objects exhibiting thermal emission in the 2.5 micron range that did not have previously measured albedos, we were able to approximate the albedo using the method in Rivkin et al. (2005) also discussed in more detail in the calculations section.

Spectral characteristics are the third important criteria for identifying comet candidates. Comet nuclei have linear spectra with neutral to red slopes, analogous to C-, P-, T-, and D-type asteroid classes. Of our Tj<3 NEOs we looked for these linear sloped spectra. S-type spectra with multiple absorption features were not considered comet candidates even if their Jovian Tisserand parameter was less than 3. We fit slopes for the

linear spectra in visible wavelengths and used these values to calculate the normalized reflectivity gradient S' as described by Jewitt (2002). We also used an infrared to visible slope conversion when only infrared data were available for certain objects. Each taxonomic type that had several objects with both visible and infrared data had its own individual conversion relation. All other types were grouped together and given a general correlation found by fitting all of the linear spectra data. This conversion is necessary to apply taxonomy rules to objects with only infrared measurements since taxonomic classes are defined only by visible data.

Observations

All observations made were spectroscopic; the near-infrared observations from 0.8 to 2.5 microns were obtained using the SpeX instrument on the 3 meter Infrared Telescope Facility (IRTF) located on top of Mauna Kea, Hawaii. When possible, objects were observed near the meridian to minimize airmass. Frames were taken so that the object was alternated between two different positions on the slit. Solar-type stars were observed to subtract the solar spectrum from the asteroid spectrum in the images. These standard stars are comparable to well established solar analogs stars such as 16 Cyg B and Hyades 64. Two to three sets of eight images were taken for each object. Exposure time for each object image was generally 120 seconds. The total exposures, therefore, near-Earth objects ranged from 30 to 120 minutes.

Visible observations out to 0.92 microns were made on the Kitt Peak National Observatory 4 meter Mayall telescope in Arizona on September 1, and December 1,

2003. Many spectra were taken from the SMASS data set. Table 1 lists all new observations.

Table 1: T<3 NEO Spectral Observation List

Object	UT Date	Telescope
3552	5-May-00	IRTF 3m
53319	11-Aug-99	IRTF 3m
65996	5-Jul-03	IRTF 3m
1999 OP3	27-Dec-02	IRTF 3m
2000 GV127	5-May-00	IRTF 3m
2000 PG3	4-Sep-00	IRTF 3m
2002 EX12	9-Jul-05	IRTF 3m
2002 XO14	27-Dec-02	IRTF 3m
2003 KP2	1-Sep-03	KPNO 4m
2003 RS1	1-Sep-03	KPNO 4m
2003 WY25	1-Dec-03	KPNO 4m
2003 XM	1-Dec-03	KPNO 4m
2004 TU12	10-Dec-04	IRTF 3m
2004 YZ23	10-Jun-05	IRTF 3m
2005 AB	12-Apr-05	IRTF 3m
2005 AT42	10-May-05	IRTF 3m

Reduction

Reduction was done using a combination of routines with the Image Reduction and Analysis Facility (IRAF), provided by the National Optical Astronomy Observatories (NOAO) (Tody 1993), and Interactive Data Language (IDL). Autospex was also used as a tool to write necessary IRAF and IDL command files.

In IRAF, images were divided by a final flat field image. AB image pairs were subtracted for sky and dark corrections. Arc images, containing the spectrum of helium, neon and argon emissions were matched with known emission wavelengths for calibration. All object frames were combined into one final image per object with the center of each 2D spectrum registered in the y-dimension and the wavelength registered

in the x-dimension. Finally the 1D spectra were extracted, and normalized with each standard star.

Using IDL, an absorption coefficient was determined for each object and star pair that best minimizes atmospheric water absorption effects for that pair. This coefficient correction is most important at the 1.4 and 2.0 micron absorption bands. The last IDL step averages all the object and standard pairs to create the final reduced spectrum for each object.

Calculations

The Jovian Tisserand value was calculated using the equation:

$$Tj = (aj/a) + 2[(1-e^2)a/aj]^{1/2}\cos(i) \qquad (2)$$

Objects 65996, 2001 ME1, 2002 EX12, 2004 YZ23, and 2005 AB were found to emit thermal radiation in the 2.0 to 2.5 micron range. By using phase angle, solar distance, and thermal excess and applying them to the templates in Rivkin et al. (2005) it is possible to obtain albedo estimates. The albedo for 2001 ME1 was calculated by Rivkin in his 2005 paper, but the albedo information for the other objects is shown in Table 2. All reflectance spectra showing thermal tails in the 2 to 2.5 micron range had low albedos ranging from 0.02 to 0.05.

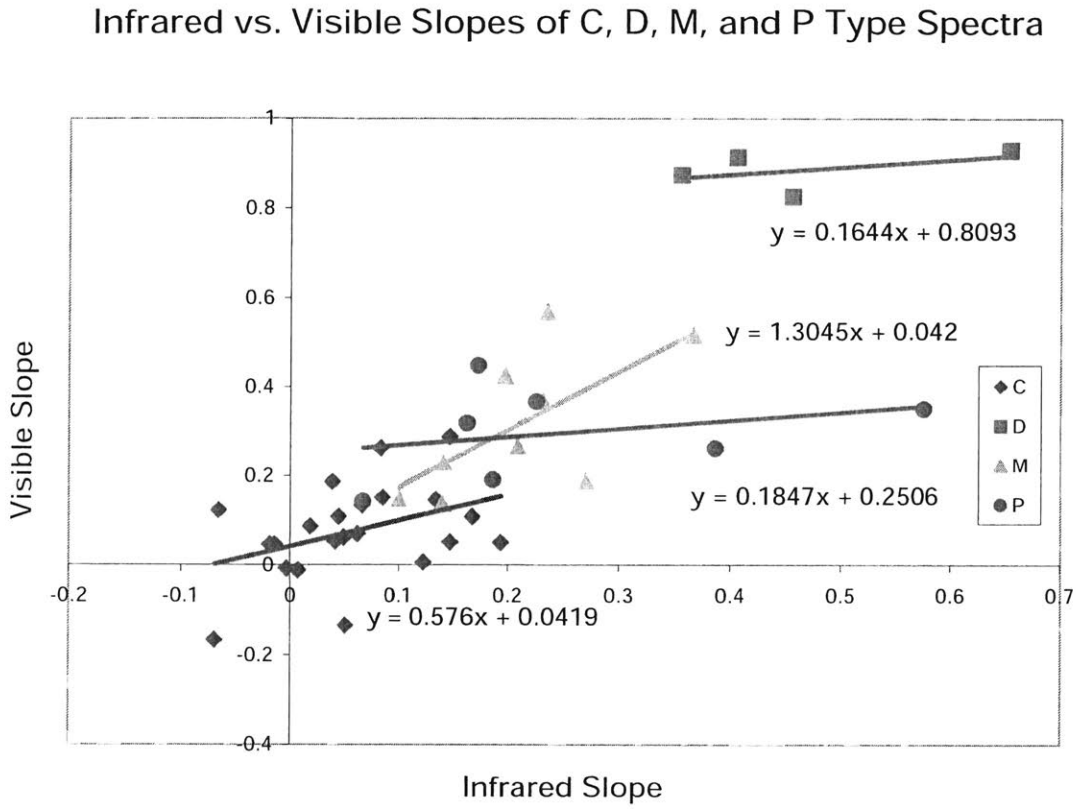

Figure 3: Plot of infrared versus visible wavelength spectra slopes for C, D, M, and P type objects with linear relations of Vis to IR for each type. This graph shows that one general correlation may not be the best fit for all types, because each type tends to have a distinct relation between its visible and infrared slopes.

Table 3: IR to Visible Slope Conversions

Type	Correlation Vis f(IR)	# fitted	R	Confidence
All	1.232x+0.0597	50	0.8406	99.7
C	0.576x+0.0419	22	0.3917	92
M	1.3045x+0.042	8	0.6907	94.7
P	0.1847x+0.2506	7	0.2980	49
D	0.1644x+0.8093	4	0.4643	44

17

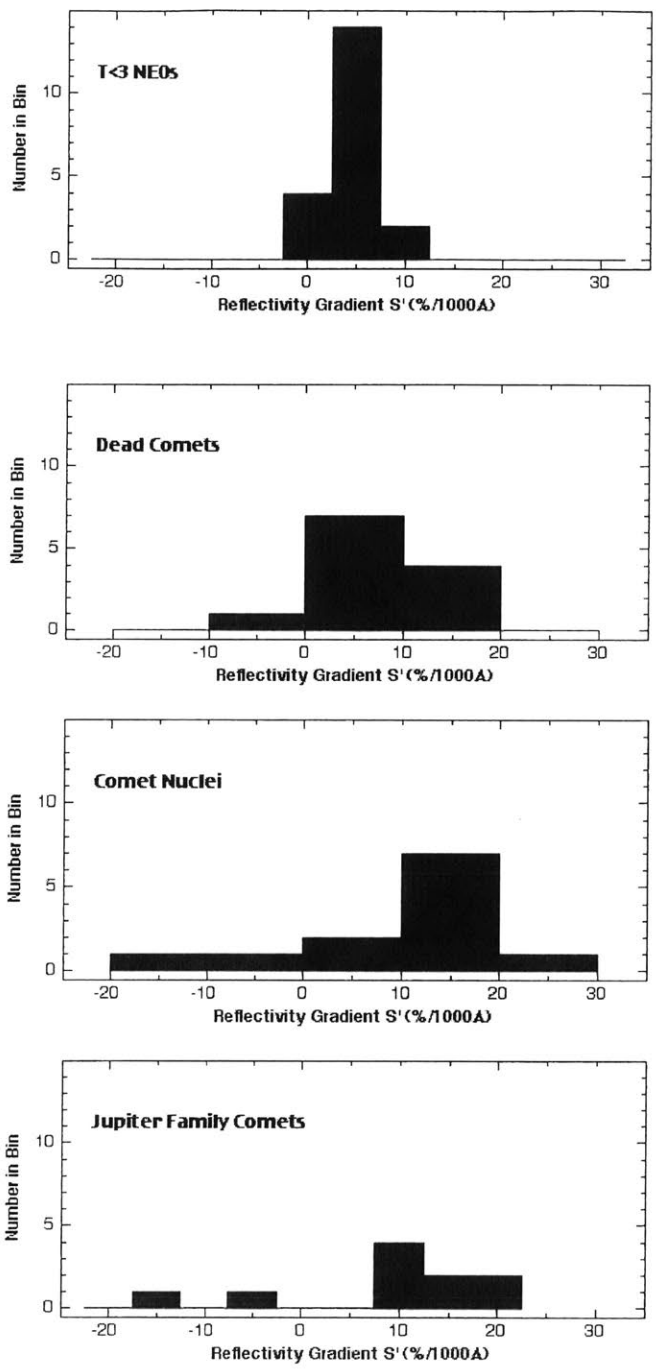

Figure 4: Graphs of frequency of reflectivity gradient values for certain object types. These graphs compare the colors of our comet-like NEOs to the color of dead comet candidates, comet nuclei, and Jupiter family comets found by Jewitt (2002, 2005).

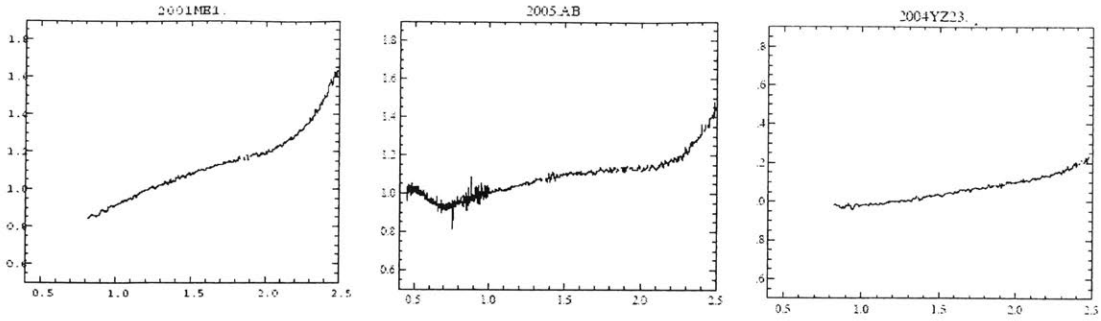

Figure 5: Plots of spectra exhibiting thermal emission at 2.5 microns.

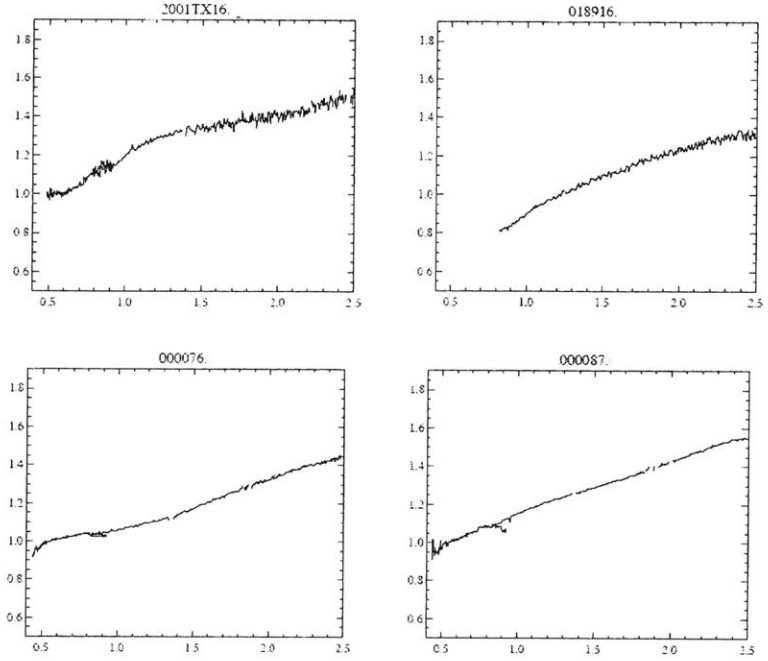

Figure 6: Plots of C, D, and T spectra. These are asteroids with comet-like spectra.

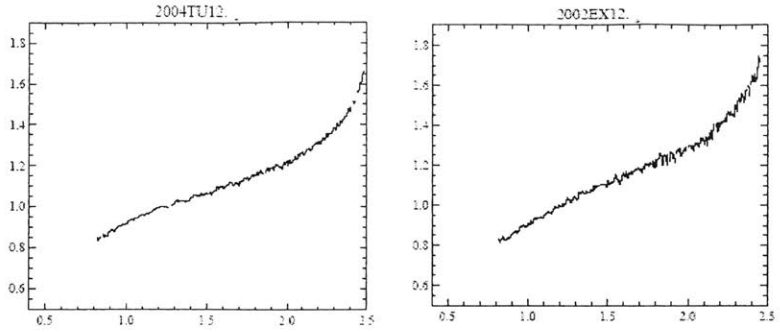

Figure 7: Plots of comet spectra. Comet spectra are linear and featureless. In our sample of T<3 NEOs, 2004 TU12, 2002 EX12, and 2003 WY25 are confirmed comets. Plotted here are spectra of 2004 TU12 and 2002 EX12. The upward curve at the end of the spectrum is due to high thermal emission because of the objects' proximity to the sun.

In Figures 5, 6, and 7 we show typical spectra for objects exhibiting thermal emission, linear spectra, and spectra of confirmed comets respectively. Their featureless spectra are all very similar, and the only distinguishing features are thermal emission and slope. We found the spectral reflectivity gradient S' for objects that have been previously published and the list of those objects can be found in Table 5. Table 6 summarizes the characteristics of all our T<3 NEOs. It lists if each spectrum is linear, if it satisfies the albedo less than 0.075 criteria when data exists. If both criteria are satisfied combined with dynamical criteria (T<3) the object is declared a comet candidate. For a complete list of all objects with their Tisserand value, S' reflectivity gradient, albedo and taxonomic class see Appendix A.

Table 5: Previously Published Objects Reported

Object	Publication
3552	1
9400	1
16960	1
85490	1
1991 XB	2
1992 UB	2
1999 DB2	1
1999 SE10	3
2000 NM	1
2000 WL10	1
2001 EC	1
2001 ME1	4
2001 SJ262	1
2001 UC5	1
2001 UU92	1
2001 YK4	1

1.Binzel et al. (2004) 2. Xu, S. (1994). Xu et al. (1995)
3. Binzel et al (2001) 4. Rivkin et al. (2005)

Table 6: S' values and comet criteria for T<3 NEOs

Object	linear	albedo<0.075	comet cand
3552	yes		yes
9400	no		no
16960	no		no
53319	yes	no**	no**
65996	yes	yes	yes
85490	yes		yes
1991 XB	no		no
1992 UB	yes	no**	no**
1999 DB2	no		no
1999 OP3	no		no
1999 SE10	yes		yes
2000 GV127	no		no
2000 NM	no		no
2000 PG3	yes		yes
2000 WL10	yes	no**	no**
2001 EC	no		no
2001 ME1	yes	yes	yes
2001 SJ262	no	no	no
2001 UC5	yes	yes**	yes**
2001 UU92	yes		yes
2001 YK4	yes	yes**	yes**
2002 EX12	yes	yes	yes*
2002 XO14	no		no
2003 KP2	yes		yes
2003 RS1	yes	yes**	yes**
2003 WY25	yes		yes*
2003 XM	yes		yes
2004 TU12	yes		yes*
2004 YZ23	yes	yes	yes
2005 AB	yes		yes
2005 AT42	no		no

*These objects are confirmed comets

**These objects are assigned albedo ranges (M or P types) based on relative frequency statistics

Table 7: JFC Source Region Probabilites from Bottke's Single Bin Method*

Object	P_JFC
3552	1.000
9400	0.000
16960	0.000
53319	0.075
65996	0.578
85490	1.000
1991 XB	0.139
1992 UB	0.412
1999 DB2	0.424
1999 OP3	0.000
1999 SE10	0.157
2000 GV127	0.120
2000 NM	0.015
2000 PG3	0.929
2000 WL10	0.926
2001 EC	0.000
2001 ME1	0.450
2001 SJ262	0.168
2001 UC5	0.000
2001 UU92	0.677
2001 YK4	0.585
2002 EX12	0.547
2002 XO14	0.109
2003 KP2	0.581
2003 RS1	0.218
2003 WY25	0.874
2003 XM	0.677
2004 TU12	0.904
2004 YZ23	0.602
2005 AB	0.268
2005 AT42	0.148

*Note: these source region probabilities were created by Bottke using his method described in Bottke et. al (2002)

In Table 7 we can see the probability of Jupiter family comets as the source region for each object in our Tj<3 object list. Note that objects 3552 and 85490 have probabilities of 1 of coming from the Jupiter Family Comet region. 2000 PG3, 2000 WL10 and 2004 TU12 also have high probabilities (P>0.9) of originating in the JFC

region. All of these objects are comet candidates according to our criteria (remember that 2000 WL10 was labeled as high albedo as a statistic and all of the X types without albedo data were arbitrarily given comet candidate status for statistical purposes).

Objects that have a zero probability of Jupiter Family Comet origins include 9400, 16960, 1999 OP3, 2001 EC, and 2001 UC5. All of these objects are rejected as comet candidates because of their non-linear spectra except for 2001 UC5. It is important to remember that 2001 UC5 just as 2000 WL10 was labeled according to statistics and it is possible that its albedo is higher than that of a comet. There is therefore no inconsistency of results between Bottke's source region model and our comet candidate criteria. For a complete list of all probabilities for all source regions including JFC, outer belt, 3:1 resonance, Mars crosser, and nu6 resonance see Appendix B.

In Figure 8 we plot the reflectivity gradient S' versus the Tisserand parameter. There does not seem to be a clear correlation, although we notice that the Tisserand parameter is generally between 2.6 and 3 for these comet-like objects that are likely to have come from the Jupiter Family Comets. There is not great diversity for this value confirming that typical Jupiter family comet objects have T between 2 and 3 and even suggesting that most have T values closer to 3.

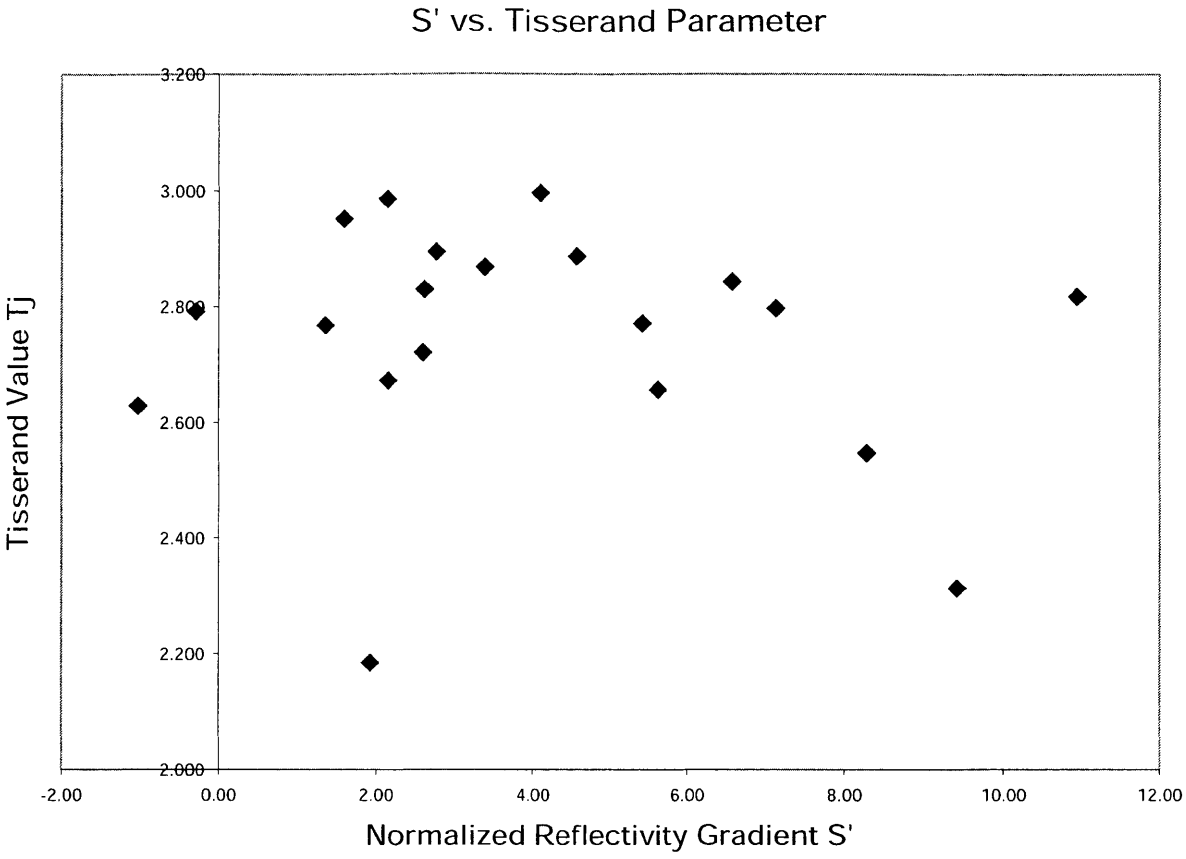

Figure 8: Normalized reflectivity gradient S' versus Tisserand parameter. This figure shows that all these comet candidates have Tj values between 2 and 3, most range between 2.6 and 3. There is no clear correlation between S' value and Tisserand value.

Discussion

For our extinct comet candidates, we find a distribution of S' values consistent with the results of Jewitt (2002) for a similar sample. In general, the colors of extinct comet candidates are less dispersed than those of active comet nuclei. The colors of our extinct comet candidates are generally consistent with the colors of Jupiter family comets.

A Jovian Tisserand parameter less than 3 is a dynamical property consistent with a possible cometary origin. Neutral to red spectral colors and low albedos are physical

properties consistent with known comets. We combine both dynamical and physical properties to estimate the possible comet fraction among NEOs.

Bias corrected discovery statistics (Stuart 2003; Stuart & Binzel 2004) show that 30% of the total NEO population resides in orbits having TJ < 3. Our observational sample of TJ < 3 NEOs reveals 17 out of 31 (55%) having colors and/or albedos consistent with comet nuclei. Taken at face value, this suggests:

$$0.30 \times 0.55 = 0.16$$

or about 16% of the total NEO population has dynamical and physical properties consistent with a cometary origin.

In the past comet-origin estimates have been lower. Dynamical estimates using theoretical models find a comet fraction of approximately 6%. (Bottke et al. 2002) Fernandez et. al (2001) found an observational estimate stating that 9% of all NEOs are comet-like. Another observational estimate was obtained by Weissman (2002) estimating that 6 +/- 4% of NEOs have the JFCs as their source region, although he notes that the number may be higher. This new observation of 16% suggests that the fraction of comet-like objects near the Earth may be slightly higher than previous estimates.

It is interesting to note that during our research two of our comet candidates, 2002 EX12 and 2003 WY25, were confirmed by other sources to be actual comets. These discoveries suggest the robustness of our method of distinguishing comet-like objects from asteroids.

Several explanations for why these comet-like NEOs are not actual comets and do not display tails are described in Weissman et. al (2002) and Jewitt (2004). Some comets lose all volatile material because of constant exposure to the sun's energy and become

extinct comets. On others ice on the surface is sublimated so that particles too massive to escape remain on the surface creating a rocky rubble mantle. This mantle prevents sunlight from reaching and heating the ice effectively isolating the ice rich nucleus underneath. A second method preventing outgasing is caused by bombardment by cosmic rays which interact with and chemically alter the surface creating an irradiation mantle. Objects that have icy cores but are protected by a mantle are called dormant comets because they can be reactivated for example by a collision.

Our list of comet-like near-Earth objects is not complete. A list of NEOs also with low albedo and Tj<3 observed by other astronomers are listed in Table 8.

Table 8: Comet-Like NEOs Observed By Other Astronomers

Object	Tisserand	Albedo	Type	Reference
14827	2.93		C	4
1983 VA	2.97	0.07 ± 0.01		2
1997 VM4	2.79		Q	4
1999 AF4	2.97		C	4
1999 LT1	2.59		C,F	4
1999 XS35	1.42	0.03		3
2000 EB107	2.84		D	4
2000 LF6	2.93		D	4
2001 RC12	2.69	0.080 ± 0.023		1

References: 1. Fernandez (2005) 2. Fernandez (1999) 3. Levinson (2002) 4. Weissman (2002)

Conclusion

We find that 16% of the total NEO population has dynamical and physical properties consistent with a cometary origin. While we recognize that the boundaries set for our criteria are in reality not definitive, we find it useful for the statistical purposes of this paper. Our value is based on 31 near-Earth objects, so to increase the robustness of

the fraction it is necessary to obtain spectra and albedos of more objects because a larger unbiased sample size will increase the accuracy of the fraction value.

It would also be useful to explore the comet fraction of other regions of the solar system. Finding comets among Mars crossing objects or even in the main asteroid belt can provide further incite into the evolution and dynamics of the solar system.

Appendix A: Comet Candidate Criteria

Object	Tisserand	S' val	Type	Location	Albedo Values	Reference	linear	albedo<0.075	comet cand
3552	2.314	9.42	D	AMO	0.045 ± 0.003	1	yes	yes	yes
9400	2.939		Sr	AMO			no		no
16960	2.999		Sq	APO			no		no
53319	2.986	2.15	X	APO			yes	no**	no**
65996	2.951	2.52	P	AMO	0.02	4	yes	yes	yes
85490	2.657	5.63	T	AMO			yes		yes
1991 XB	2.934		K	AMO			no		no
1992 UB	2.895	2.77	X	AMO			yes	no**	no**
1999 DB2	2.901		Sq	AMO			no		no
1999 OP3	2.932		S	AMO			no		no
1999 SE10	2.844	6.59	D	AMO			yes		yes
2000 GV127	2.940		S	AMO			no		no
2000 NM	2.932		Sr	APO			no		no
2000 PG3	2.547	-1.40	D	APO	0.046 ± 0.012	2	yes	yes	yes
2000 WL10	2.722	2.60	Xc	APO			yes	no**	no**
2001 EC	2.910		Sq	APO			no		no
2001 ME1	2.673	2.59	P	APO	0.04	3	yes	yes	yes
2001 SJ262	2.976		C:	AMO	0.177 ± 0.051	2	no	no	no
2001 UC5	2.869	3.38	X	AMO			yes	yes**	yes**
2001 UU92	2.798	7.15	D	AMO			yes		yes
2001 YK4	2.831	2.62	X:	APO			yes	yes**	yes**
2002 EX12	2.887	4.58	T	APO	0.03	4	yes	yes	yes*
2002 XO14	2.980		S	APO			no		no
2003 KP2	2.629	-1.03	C	APO			yes		yes
2003 RS1	2.996	4.11	X	AMO			yes	yes**	yes**
2003 WY25	2.818	10.95	D	APO			yes		yes*
2003 XM	2.772	5.43	T	AMO			yes		yes
2004 TU12	2.792	3.76		JFC			yes		yes*
2004 YZ23	2.184	2.55	P	AMO	0.05	4	yes	yes	yes
2005 AB	2.792	-0.29***	C	AMO	0.04	4	yes	yes	yes
2005 AT42	2.969		S	AMO			no		no

*These objects are confirmed comets
**These objects are assigned albedo ranges (M or P types) based on relative frequency statistics and do not reflect that specific objects albedo.
***Visible data provided by P. Vernazza (Obs. Paris Meudon)
References: 1. Fernandez (1999) 2. Fernandez (2005) 3. Rivkin et al. (2005) 4. this work

Jewitt, D.C. (2005). A first look at damocloids. AJ, 129, 530.

Lamy, P.L, Toth, I., Fernandez, Y.R., Weaver, H.A., (2004) The sizes, shapes, albedos, and colors of cometary nuclei. In Comets II, (M. Festou, H. Weaver, H. Keller, eds.) Univ. Arizona Press, pp. 223-264.

Lebofsky, L. A., Spencer, J. R. (1989). Radiometry and thermal modeling of asteroids. In Asteroids II, (R. P. Binzel, T. Gehrels, M. Matthews, eds.), Univ. Arizona Press, pp. 128-147.

Rivkin, A.S., Binzel, R.P., Bus, S.J. (2005). Constraining near-Earth object albedos using near infrared spectroscopy. Icarus 175, 175.

Stuart, J.S. (2003). Observational constraints on the number, albedos, sizes, and impact hazards of the near-Earth asteroids. Doctoral thesis. Massachusetts Institute of Technology, Cambridge, Massachusetts.

Stuart J.S., Binzel, R.P., (2004) Bias-corrected population, size distribution, and impact hazard for the near-Earth objects. Icarus 170, 295. Tedesco, E.F., Dennis, L.M., Veeder, G.J., (1989). Classification of IRAS asteroids. In Asteroids II, (R. P. Binzel, T. Gehrels, M. Matthews, eds.), Univ. Arizona Press, pp 290-297.

Tody, D. (1993) IRAF in the Nineties. In Astronomical Data Analysis Software and Systems II (R. J. V. Brissenden, and J. Barnes, Eds.), pp 173. Astron. Soc. Of the Pacific, San Francisco.

Weissman, P.R., Bottke, W.F., Levison, H.F., (2002) Evolution of comets into asteroids. In Asteroids III, (W.F. Bottke, A.Cellino, P. Paolicchi, R.P. Binzel eds.), Univ. Arizona Press, pp. 669-686.

Wetherill, G.W., (1988) Where do the Apollo objects come from? Icarus 76, 1.

Wisdom, J., (1985) Meteorites may follow a chaotic route to Earth. Nature 315, 731.

Xu, S. (1994). CCD Photometry and Spectroscopy of Small Main-Belt Asteroids. Ph. D. Thesis, Massachusetts Institute of Technology.

Xu, S., Binzel, R. P., Burbine, T. H., and Bus, S. J. (1995). Small Main-Belt Asteroid Spectroscopic Survey: Initial Results. Icarus 115, 1-35, 1995.